LIDAR SENSOR FOR MEASURING DIRECTIONAL-SPECTRAL CHARACTERISTICS OF WATER WAVES

Jennifer L. Irish[1], Jennifer McClung Wozencraft[2], and A. Grant Cunningham[3]

1. U.S. Army Engineer Research and Development Center, Coastal and Hydraulics Laboratory, Joint Airborne Lidar Bathymetry Technical Center of Expertise, OP-J, 109 St. Joseph Street, Mobile, AL 36602-3630 USA, Tel.: 334-690-3465, Fax: 334-690-3464, Email: jennifer.l.irish@usace.army.mil
2. U.S. Army Corps of Engineers, Joint Airborne Lidar Bathymetry Technical Center of Expertise, Mobile, AL USA
3. Optech Incorporated, North York, Ontario, Canada

ABSTRACT

Conventional *in situ* wave gages, like the pressure gage and current meter (PUV) and the directional wave gage (DWG), cannot satisfy all water-wave measurement requirements in the coastal zone. Specifically, new measurement technologies are required to allow for wave measurement within navigation channels and near navigation structures where bottom-mounted gages are not easily deployed or may themselves become hazards to navigation. Bottom-mounted wave gages do not directly measure the elevation of the water surface. Instead, these measurements approximate water surface elevation based on other hydrodynamic processes. The results can be faulty if these processes are different than assumed during analysis. In December 1999, a non-intrusive directional lidar wave gage (LWG) was tested. The LWG uses lidar technology to directly measure water surface elevation. So unlike bottom-mounted gages, the surface elevation measurement from the LWG is independent of other hydrodynamic processes. The prototype LWG consists of four rangefinders, a compass, and an inclinometer. Each rangefinder collected water surface elevation time series at a rate of 10 Hz. The laser footprints were positioned to form an approximate 1-m square. The compass and inclinometer allowed for accurate positioning of the footprints on the water surface. Throughout the field test, ground truth was collected concurrently with the LWG data using a PUV mounted directly beneath the LWG. Directional-spectral wave characteristics determined from the LWG time series using standard Fourier analysis procedures match well with PUV results. This paper discusses the technology on which the LWG is based and presents the preliminary results from the field test of the prototype sensor.

INTRODUCTION

Accurate meaningful wave measurements within the coastal regime, particularly at coastal navigation projects, are extremely hard to obtain with present technology. Due to the severity of the physical environment and the difficulty of properly characterizing the radical changes that take place within the spatial wave field, new wave measurement technologies are needed to augment existing *in situ* methods (1, 2). Oftentimes, bottom-mounted gages are not easily deployed or may themselves become hazards to navigation. Further, the performance of *in situ* wave gages is limited in the presence of strong currents. Consequently, little or no high-quality information exists for wave characteristics in nature related to hazardous navigation conditions. Trapped waves, wave breaking (both depth and current induced), and wave-current interaction are not well understood at present. Because of limited field measurement capabilities, hydrodynamics models designed to predict wave conditions at navigation projects are still largely untested in the field. Further, systems used for channel design, such as ship simulators, must rely on relatively crude approximations of the conditions actually encountered by ship's pilots. It is essential to have high-quality field measurements in order to test, verify, and understand the limitations of different theoretical and numerical approximations, if such models are to be used for coastal engineering and management. Project-specific input to a channel design system will always be only as good as the ability to measure project conditions.

In December 1999, a non-intrusive directional lidar wave gage (LWG) was tested. The LWG uses lidar technology to directly measure water surface elevation. So unlike bottom-mounted gages, the surface elevation measurement from the

LWG is independent of other hydrodynamic processes. The prototype LWG consists of four rangefinders, a compass, and an inclinometer. Each rangefinder collected water surface elevation time series at a rate of 10 Hz. The laser footprints were positioned to form an approximate 1-m square. The compass and inclinometer allowed for accurate positioning of the footprints on the water surface. Throughout the field test, ground truth was collected concurrently with the LWG data using a PUV mounted directly beneath the LWG. Directional-spectral wave characteristics determined from the LWG time series using standard Fourier analysis procedures match well with PUV results. The following sections discuss the technology on which the LWG is based and presents the preliminary results from the field test of the prototype sensor.

LWG CHARACTERISTICS AND FIELD EXPERIMENT SETUP

The prototype LWG consists of two main segments: a sensor platform and a data acquisition suite. Figure 1 shows the LWG principle of operation. The instrument is designed to facilitate quick and easy adjustments to the positioning and spot (laser footprint on water surface) spacing of the laser measurements. The sensor platform contains four model SLX-3A rangefinders, using time-of-flight ranging technology, that were programmed for the purpose of recording and transmitting remote range measurements to a personal computer (PC). Each rangefinder field of view (FOV) is folded 90° by a steering mirror. Each steering mirror is adjustable to allow translation of the laser FOV on the target surface over an approximate ±12 deg. range relative to off-nadir[1]. Each mirror mount has two micrometer dials for orthogonal movement and is calibrated so accurate spot patterns can be achieved by selecting the appropriate dial settings. This allows for quick changes in pattern without calibrations in the field. The rangefinders transmit and receive through glass windows so that the enclosure can be sealed to moderate weather. Access to the mirror adjustments is through a removable weather-sealed cover.

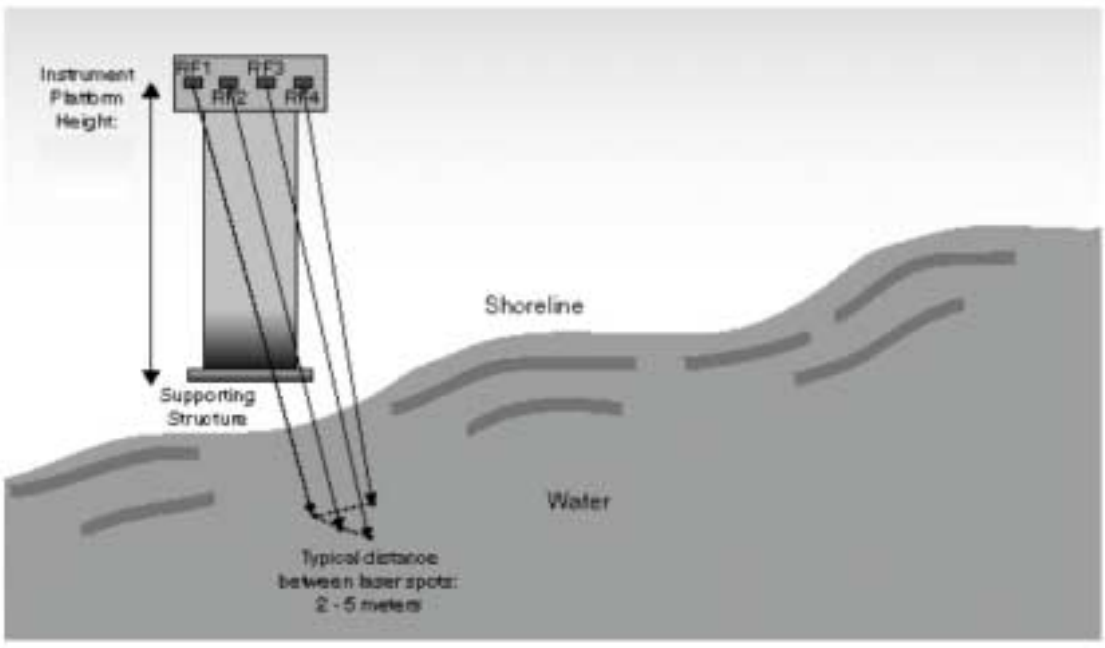

Figure 1: LWG principle of operation.

The sensor platform has an electronic compass with direction (heading) and attitude outputs. This provides accurate positioning information of the spot pattern. The accuracy of the compass is ±0.5 deg. and the attitude sensors are ±0.2 deg. In addition to being able to adjust the spot spacing, the entire sensor platform may be rotated about its longitudinal axis more that 45 deg. forward and back. The angle can be set to within a degree or two using dial readouts on the outside of the enclosure. The compass module provides the final attitude of the platform once it is in place.

[1] off-nadir angle is measured from vertical, where 0 deg. is directly down-looking.

Communications with the rangefinders and compass are through an RS-232 serial twisted-pair shielded cable. The data acquisition suite consists of a PC and a 24V DC power supply to provide the sensor-platform with power. The PC is a Pentium II, 400MHz, 64MB SDRAM, 6.4GB hard disk drive, running Microsoft Windows98, Second Edition operating system. The instrument-specific software was generated using Visual C++ 6.0 integrated development environment. Installed in the PC is a multi-port adapter card that adds four additional serial ports. The rangefinder microprocessors communicate with the PC through this card. A timer/counter card was also installed in the PC to provide timing and simultaneous trigger signals for the four rangefinders.

The sensor platform is designed to mount directly onto the end of the USACE Coastal and Hydraulics Laboratory Field Research Facility's (FRF) Sensor Insertion System (SIS) upper boom (Figure 2) (3). A Lambda DC power supply is located with the PC to supply power to the sensor platform. All of the data acquisition equipment will use the available 110 VAC, 60 Hz commercial power in the enclosure on the SIS truck, located forward of the SIS crane. The sensor platform and data acquisition connection is by a single 150-m cable that runs from the sensor along the SIS upper boom to the PC inside the SIS truck.

Figure 2: SIS deployed with LWG on north side of FRF pier.

Field experiments of the prototype LWG were conducted at the FRF 5 – 17 December 1999. A pressure gage and current meter (PUV) gage was positioned on the SIS lower boom to provide ground truth measurements (Figure 2). Each LWG data record consisted of (x, y, z) time series at 4 locations (RF1, RF2, RF3, and RF4) positioned to form a rectangle with spacing varying from 0.6 m to 2.0 m. The rangefinder measurement positions relative to the LWG are shown in Figure 3. Figure 4 shows a sample time series of water level elevation for all four rangefinders. Additional data sets were collected specifically to quantify the LWG sensitivity to environmental conditions and sensor settings

.

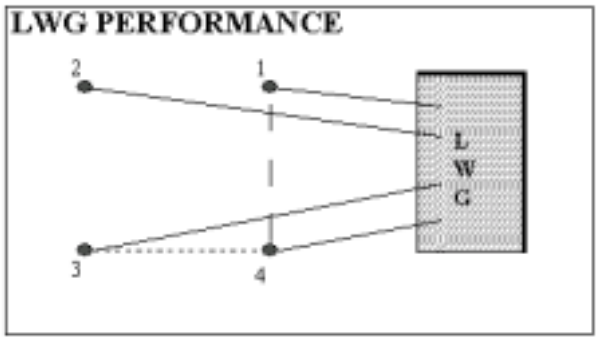

Figure 3: LWG rangefinder (RF1 through RF4) horizontal measurement location.

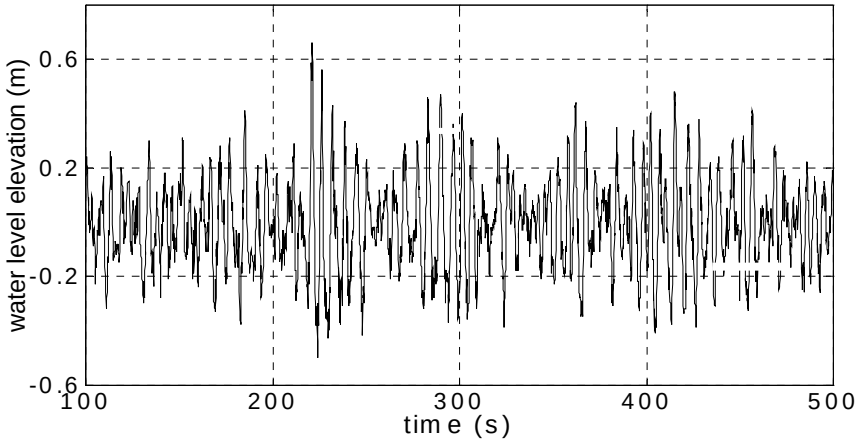

Figure 4: Sample water surface elevation time series.

Field data records were collected over a variety of sea-surface conditions. Wave height varied from 0.2 m to 1.5 m and varied in type from one-directional clean swell to choppy seas. Because the LWG measures water surface elevation by ranging obliquely to the surface, the measured horizontal position varies with time. The rangefinder slant range measurements collected by the sensor were processed and resulted in an x-y-z position measured 10 times per second (Figure 5). The figure shows the data in two dimensions to demonstrate the horizontal variability in the spot location for all four rangefinders. The field experiment confirmed that the magnitude of this movement is directly related to wave height. Notice that the variability in (x, y) is greater in Figure 5b, where the wave height is larger, than in Figure 5a, where the wave height is smaller.

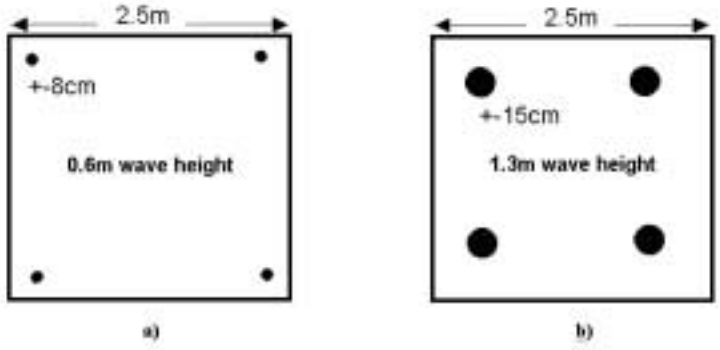

Figure 5: Horizontal variation in spot position for waves with a mean height of a) 0.6 m and b) 1.3 m.

Data were collected under a range of ambient light conditions, derived from time of day, and weather conditions. Weather conditions ranged from sunny and clear to overcast skies. A few tests were run during periods of light to moderate rain. As the sensor was not fully weatherproofed, no tests were run during periods of heavy rain. While some water damage resulted from heavy rain because the LWG casing was not fully weatherproofed, the technology's performance was not significantly impacted by the range of light and rain conditions encountered during the field experiment.

It became obvious early in the experiment that success of the LWG in receiving a suitable return signal from the water surface was largely dependent on the presence of capillary waves. These waves provided a roughness on the water surface from which the lidar signal was scattered back to receivers in the sensor. Because the presence of capillary waves is directly a function of wind speed, the LWG performance is a function of wind speed (Figure 6a). In the figure, a dropout refers to lidar pulses not returned from the water surface to receivers in the LWG. Each point on the figure represents the percentage of lidar pulses not returned for a data record consisting of 16 minutes of continuous data collection at 10 Hz. For example, the uppermost circle on the figure (where wind speed is about 1.5 ms^{-1}) indicates an 80% loss of data during this 16-minute collection duration. The figure shows the percentage of dropouts is less variable at higher wind speeds.

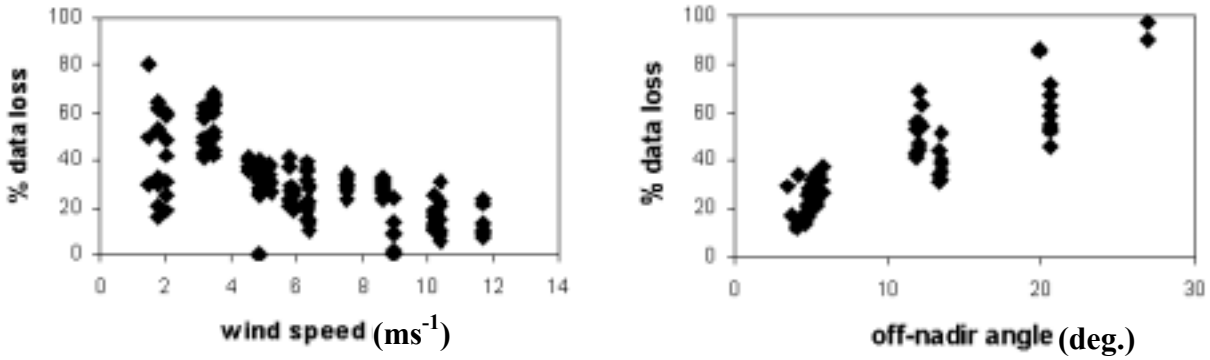

(a) **(b)**

Figure 6: Percent of data dropouts relative to a) wind speed for data collected on 9, 10, and 14 December (off-nadir angle was less than 15 deg.) and b) off-nadir angle on 13 December (wave height was less than 1 m and wind speed was 5-10 ms^{-1}).

During the field experiment, a range of off-nadir angles and sensor elevations above the water surface were tested. Ranging distances to the water surface varied from 6 m to 16 m. The field results show that within this elevation range, sensor performance remains constant. In contrast, off-nadir angle variation significantly impacts the LWG performance. Data were collected for off-nadir angles ranging from 0 to 30 deg. (Figure 6b). As expected, the number of dropouts increases with an increase in off-nadir angle. These findings indicate that a LWG will perform best when off-nadir angles are less than 10 deg. and wind speeds are greater than 5 ms^{-1}.

DATA QUALITY AND PRE-PROCESSING

During spectral analysis (see following sections) of the LWG data, suspicious results were encountered. Wave directions computed using the full 16-minute data record produced seemingly random results with no correlation with the wave direction calculated from the PUV gage data. However, wave directions computed from the first half of each data record (8 minutes of data) showed reasonable agreement with the PUV results. In contrast, wave directions computed from the second half of each data record showed significant deviations from the PUV results. This indicates that for each data record, the reported (x, y, z) became corrupted toward the end of the collection period. To date, the exact cause of this data corruption is undetermined. However, existing hypotheses consider problems related directly to specific hardware and/or software issues and are not related to the theory and technology on which the LWG is based.

For the remainder of analyses presented herein only the first 8 minutes of each data record is used. A total of 60 data records were processed using spectral analysis and compared with PUV results.

SPECTRAL ANALYSIS - THEORY

Preliminary calculation of peak wave height, period and direction was performed using standard spectral analysis techniques (4, 5). For each of the four rangefinders, the data record consisted of 4096 (x, y, z) measurements. In this preliminary analysis phase, we assumed x-y variation negligible, thus reducing each rangefinder's time series to a measurement of water surface elevation, or z, only. Once the data mean and trends were removed, the data record was divided into 15 segments with a 50% overlap between segments, with each segment containing 512 measurements. Once analysis was completed for each of the 15 segments, their results were averaged to produce the final result for the data record.

Spectral wave characteristics are derived from Fourier analysis of the data records, specifically the calculation of the auto- and cross-correlation functions:

$$\Phi_{nm} = \sum_{1}^{N} F_m F_n^* \tag{1}$$

where Φ_{nm} is the auto-correlation when n=m and the cross-correlation when n≠m for each frequency; F is the Fourier transform (into the frequency domain) of the time series; and * represents the complex conjugate. The non-directional power spectral density function (S) for each frequency is represented as:

$$S(i) = 2N\Delta t \Phi_{nn}(i) \tag{2}$$

where i represents each frequency, N is the number of measurements in each segment, and Δt is the time interval between measurements. The peak frequency, f_p, is taken as the frequency corresponding to the maximum of S. Peak wave period is the inverse of f_p. The spectral wave height (H_{mo}) is computed from the first spectral moment of S:

$$H_{mo} = \frac{4}{N\Delta t}\sqrt{\sum_{i}^{I} S_{nn}(i)} \tag{3}$$

A preliminary estimate of wave direction is found by calculating the directional wave number using three of the four rangefinder time series. Below, the equations for calculating the x- and y- components of the directional wave number (k_x and k_y, respectively) for each frequency are shown using RF1, RF2, and RF3 (see Figure 3):

$$k_x = \frac{\Delta\theta_{23}\Delta y_{12} - \Delta\theta_{21}\Delta y_{32}}{\Delta x_{32}\Delta y_{12} - \Delta x_{12}\Delta y_{32}} \tag{4}$$

$$k_y = \frac{\Delta\theta_{21} - k_x\Delta x_{12}}{\Delta y_{12}} \tag{5}$$

where $\Delta y_{12} = y_1 - y_2$, $\Delta y_{32} = y_3 - y_2$, $\Delta x_{12} = x_1 - x_2$, $\Delta x_{32} = x_3 - x_2$, and the phase shift ($\Delta\theta_{nm}$) is defined as:

$$\Delta\theta_{nm} = \tan^{-1}\left\{\frac{\mathrm{Im}(\Phi_{nm})}{\mathrm{Re}(\Phi_{nm})}\right\} \tag{6}$$

The wave direction is calculated as:

$$\Theta = \tan^{-1}\left\{\frac{k_y}{k_x}\right\} \tag{7}$$

The relationship in Eq. 7 is evaluated for the peak frequency derived from S.

SPECTRAL ANALYSIS - RESULTS

Figure 7 shows representative non-directional power spectral density versus frequency as calculated by Eq. 2. In each plot, S is shown for each of the four laser rangefinders, RF1 through RF4, and for the results calculated for the PUV gage. In most instances, there is consistency between the spectra for all four rangefinders. These figures show some discrepancies between the LWG spectra and the PUV spectra. The exact nature of this discrepancy has yet to be determined. Some possible reasons for the discrepancy include measurement in slightly different locations and differences in data processing techniques. In addition, the PUV and LWG measure water surface elevation differently: the PUV correlates a measured pressure with the water surface elevation whereas the LWG directly ranges the distance to the water surface.

While there are some discrepancies between the calculated power spectra for the PUV and the LWG, the spectral wave characteristics compare well. Figure 8 shows f_p for the LWG versus that for the PUV. The frequency bandwidth used in this analysis is 0.0312 s^{-1}. With the exception of 2 records, all of the LWG results fall within one bandwidth of the PUV results. Spectral wave heights measured with the LWG match well with those measured by the PUV. This comparison is shown graphically in Figure 9.

In Figure 10, averaged wave directions calculated from LWG measurements using Eqs. 4 through 7 are plotted against those calculated from the PUV measurements. The figure represents the average of the four separate calculations made from the LWG data. Each calculation was based on the plane formed between three of the four rangefinder measurements. The figure shows that the LWG wave directions correlate fairly well with the PUV wave directions. No correlation between wave direction accuracy and either spot patterns or x-y deviations was found. Figure 11 shows the standard deviation of wave direction measured by the LWG from that measured by the PUV as it is impacted by wave height. The figure shows that for all 60 data records (H > 0.0 m), more than 90% of mean calculated LWG directions fall within 20 deg. of the PUV wave directions. As expected, the LWG performs better for larger wave heights, and for wave heights 1 m or greater, 90% of the LWG directions fall within 12 deg. of that measured by the PUV.

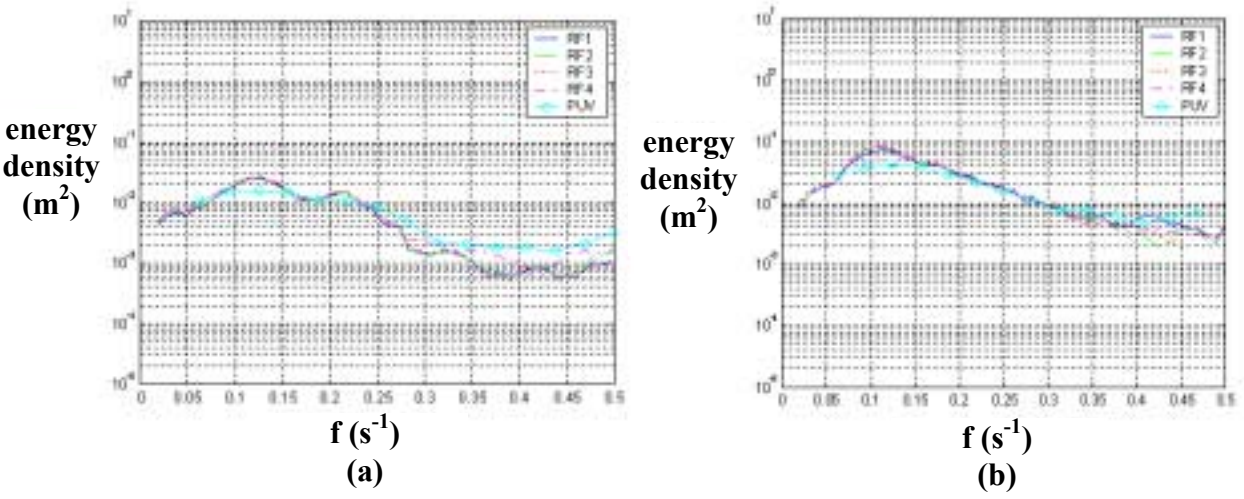

Figure 7: Non-directional spectra for a) 9 December and b) 13 December.

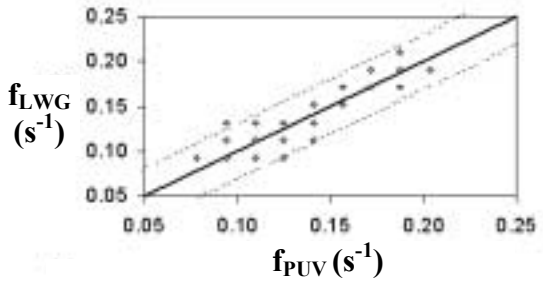

Figure 8: LWG peak wave frequency.

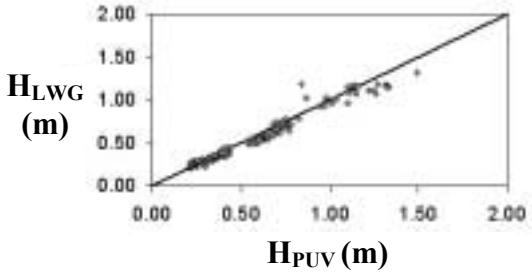

Figure 9: LWG first-moment wave height.

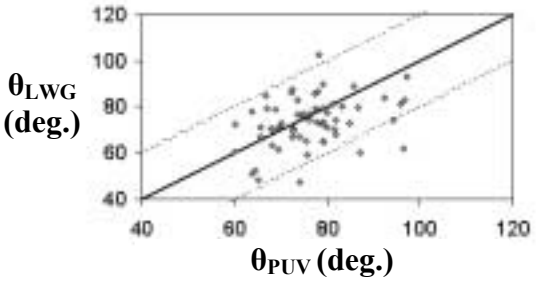

Figure 10: LWG direction in degrees (from which waves are coming, relative to true north).

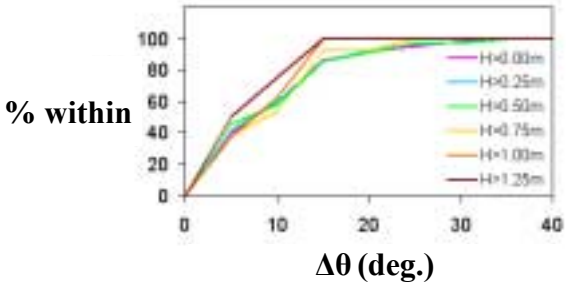

Figure 11: Wave direction deviation from wave direction measured by PUV as a function of wave height.

CONCLUSIONS

These results indicate that direct lidar ranging is a viable method for measurement of coastal waves. Figure 12 illustrates combining laser and *in situ* wave measurement techniques to establish a comprehensive monitoring program for a complex area, such as East Pass, Florida, USA, shown in the figure.

The spectral analyses presented herein are preliminary, and we expect that a more comprehensive analysis procedure will provide more accurate and reliable results. Future investigations will assess other spectral parameters, such as mean frequency. Additionally, other analysis techniques, such as the maximum likelihood method, will be considered for the calculation of wave direction.

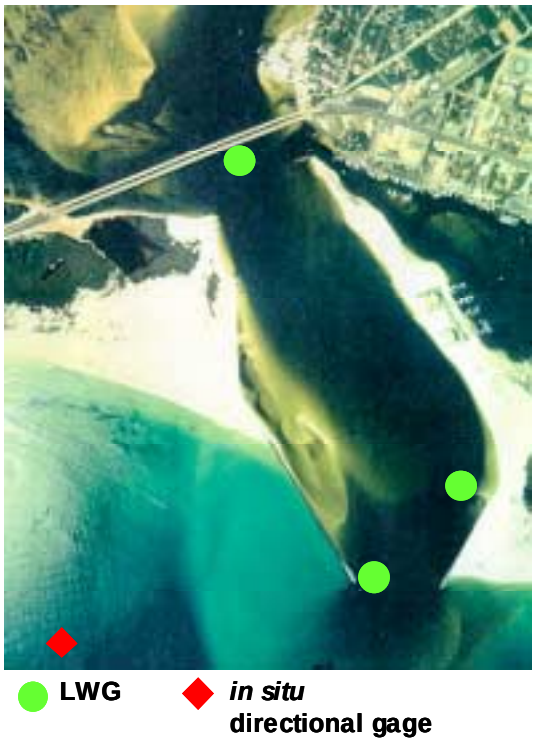

Figure 12. Conceptual wave measurement scheme combining lidar with *in situ* methods.

ACKNOWLEDGEMENTS

The authors would like to thank Mr. Carl Miller and the entire U.S. Army Engineer Field Research Facility staff for their support of field operations and analysis of control measurements. The projects, analyses, and resulting data described herein, unless otherwise noted, were obtained from work funded by or performed at the Engineering Research and Development Center of the U.S. Army Corps of Engineers. The use of trade names does not constitute an endorsement in the use of these products by the U.S. government. Permission was granted by the Chief of Engineers to publish this work.

REFERENCES

1. Howell, G. L. 1998. Shallow water directional wave gages using short baseline pressure arrays. Coastal Engineering. 35(1-2): 85-102.
2. Horikawa, K., ed. 1988. Nearshore dynamics and coastal processes. (University of Tokyo Press)
3. Leffler, M. W., Baron, C. F., Scarborough, B. L., Hathaway, K. K., Hodges, P. R., Townsend, C. R. 1996. Annual data summary for 1994 CERC Field Research Facility. TR CERC-96-6. U.S. Army Corps of Engineers.
4. Kirby, J. T. 1998. Analysis of regular and random ocean waves. Course notes for University of Delaware course #CIEG681.
5. Earle, M. D., McGehee, D., and Tubman, M. 1995. Field wave gaging program, wave data analysis standard. IR CERC-95-1. U.S. Army Corps of Engineers.